# Dynamical effects from anomalies: Modified electrodynamics in Weyl semimetals

Xuzhe Ying,[1,2] A. A. Burkov,[1,2] and Chong Wang[2]
[1]*Department of Physics and Astronomy, University of Waterloo, Waterloo, Ontario, Canada N2L 3G1*
[2]*Perimeter Institute for Theoretical Physics, Waterloo, Ontario, Canada N2L 2Y5*

(Received 18 October 2022; revised 13 December 2022; accepted 10 January 2023; published 18 January 2023)

We discuss the modified quantum electrodynamics from a time-reversal-breaking Weyl semimetal coupled with a $U(1)$ gauge (electromagnetic) field. A key role is played by the soft dispersion of the photons in a particular direction, say $\hat{z}$, due to the Hall conductivity of the Weyl semimetal. Due to the soft photon, the fermion velocity in $\hat{z}$ is logarithmically reduced under renormalization group flow, together with the fine-structure constant. Meanwhile, fermions acquire a finite lifetime from spontaneous emission of the soft photon, namely, the Cherenkov radiation. At low-energy $E$, the inverse of the fermion lifetime scales as $\tau^{-1} \sim E/\mathrm{PolyLog}(E)$. Therefore, even though fermion quasiparticles are eventually well-defined at very low energy, over a wide intermediate energy window the Weyl semimetal behaves like a marginal Fermi liquid. Phenomenologically, our results are more relevant for *emergent* Weyl semimetals, where the fermions and photons all emerge from strongly correlated lattice systems. Possible experimental implications are discussed.

DOI: 10.1103/PhysRevB.107.035131

## I. INTRODUCTION

Weyl fermions, since their original proposal, have been widely studied due to their chiral nature [1–9]. In the recent decades, much focus has been put on the condensed matter realization, namely, the Weyl semimetal (WSM) [7–10]. In Weyl semimetals, due to the separation of Weyl fermions in momentum space, various intriguing phenomena have been observed, e.g., the Fermi arc [8,9], the anomalous Hall effect [7,11], the quantized circular photogalvanic effect [12], etc. The dynamical properties of WSMs have also attracted much attention [13–16]. While a magnetic Weyl semimetal is typically subject to weak interaction of a particular form (short-ranged or Coulomb), an emergent WSM is a more versatile playground for studying interaction effects, e.g., topological orders in three dimensions [17–19], generalizations of the standard QED [20], etc.

An emergent WSM is a strongly interacting lattice system of spins or electrons, of which the low-energy effective theory is described by an emergent $U(1)$ gauge field (or some $\mathbb{Z}_m$ descendent) coupled to a WSM formed by emergent fermions. In spin liquid terminology, these are $U(1)$ (or $\mathbb{Z}_m$) spin liquids with spinon Weyl semimetals. Unlike in ordinary Weyl semimetals, the emergent Weyl fermions could naturally have a velocity close to that of the $U(1)$ gauge field, and the gauge coupling strength (fine-structure constant) does not have to be small at a given energy scale. The possibility of an emergent WSM phase has been demonstrated in Refs. [17,21–24]. The emergent WSM phase has further been proposed to be the parent state of topological orders in three dimensions [17–19]. While the descendent topologically ordered phases are stable by the formation of many-body gaps, the properties of the emergent WSM phase itself are largely studied at the mean-field level. In particular, the dynamical consequences of gauge fluctuations in emergent WSMs remain unexplored.

In this work, we focus on the case with the emergent $U(1)$ gauge field, also referred to as the emergent electromagnetic (EM) field. One important notion in studying the WSM phase is the unquantized anomaly, which guarantees the gaplessness of the WSM [11,25–27]. When an EM field emerges, the dynamical aspect of the anomalies is also an important piece of information. The unquantized anomaly appears as a Chern-Simons-like action in $(3+1)$ dimensions [11,25–27]. Together with the Maxwell action, the modified electrodynamics is usually referred to as Carroll-Field-Jackiw electrodynamics [20]. In the modified electrodynamics, the physical polarization of propagating photons is different from that of those in the vacuum. Another important feature is the anisotropy. In particular, one of the photon modes becomes soft in a particular direction [20]. Emergent photons with similar features have also been found in the coupled layers of Laughlin states [28].

In this article, we study the interplay between the fermionic degrees of freedom and the modified electrodynamics in an emergent WSM. The situation under consideration is really a simple, non-Lorentz-symmetric generalization of textbook QED, but with unconventional outcomes. Indeed, we will show that due to the interaction with the soft photons, the emergent WSM represents an unconventional quantum liquid.

More specifically, the presence of soft photons significantly influences the low-energy properties of the fermions. There are two major results. First, the fermion dispersion is strongly dressed by the photons. Namely, the fermion velocity in the soft photon direction is reduced to zero under the renormalization group (RG) flow. Besides, the system flows to a noninteracting limit under the RG. Second, fermions can spontaneously emit photons. As a result, the fermions acquire a finite lifetime, due to the Cherenkov radiation of the soft photons, that is inversely proportional to the fine-structure

 

constant and the fermion energy. The two effects just mentioned make the emergent WSM significantly different from the free WSM or the standard QED. Indeed, over a wide energy window, the emergent WSM behaves like a marginal Fermi liquid due to the finite lifetime [29]. Meanwhile, the infrared behavior shows an asymptotic two-dimensional character and is well-controlled under the RG flow. Hence, the emergent WSM represents an unconventional type of quantum liquid. Lastly, we propose that the reported feature of an emergent WSM can be observed from the specific heat measurement at low temperature [30,31].

The rest of the article is organized as follows. Section II reviews the low-energy description of a Weyl semimetal as well as the modified electrodynamics. A physical picture is developed for the dynamical effects. Section III is devoted to quantum mechanical one-loop-diagram calculations, from which the RG flow and the fermion lifetime can be obtained. Section IV concludes the article and discusses the possible experimental implications. Supplemental Material [32] is provided for the technical details in Sec. III.

## II. (EMERGENT) WEYL SEMIMETAL AND MODIFIED ELECTRODYNAMICS

In this section, we review the low-energy description of the fermions and the modified electrodynamics in an emergent Weyl semimetal (WSM) at the mean field level. A qualitative picture for the dynamical effects is provided.

The mean field description of the emergent WSM starts with a parton decomposition, which formally corresponds to fractionalizing the electron annihilation operator $c$ into a neutral fermion (spinon, $\psi$) and a charged boson (chargon, $e^{i\theta_c}$): $c = e^{i\theta_c}\psi$ [33]. The local $U(1)$ gauge ambiguity of this decomposition,

$$\psi \to e^{i\alpha}\psi, \quad e^{i\theta_c} \to e^{-i\alpha}e^{i\theta_c}, \tag{1}$$

dictates the necessity of the emergence of a dynamical $U(1)$ gauge field [34]. In other words, there is a dynamical $U(1)$ gauge field that couples to both the the spinon and the chargon with gauge charge $q = \pm 1$. We then consider mean field states in which the chargons $e^{i\theta_c}$ are gapped (and therefore can be integrated out at low energy), while the spinons $\psi$ form a Weyl semimetal band structure, with two Weyl cones of the opposite chirality separated in momentum space by $2\boldsymbol{Q}$ [see Fig. 1(a)].

At low energy, the fermionic excitation of a Weyl semimetal is effectively described by a Dirac Lagrangian [11]:

$$\mathcal{L}_{\rm f} = \bar{\psi}\, \mathcal{V}^\mu i\partial_\mu \psi, \text{ with } \mathcal{V}^\mu = [\gamma^0, \gamma^1, \gamma^2, v_3\gamma^3], \tag{2}$$

where $\gamma^{0,1,2,3}$ are the $4\times 4$ $\gamma$ matrices satisfying $\{\gamma^\mu, \gamma^\nu\} = 2\eta^{\mu\nu}$ and $\eta^{\mu\nu} = \mathrm{Diag}[1,-1,-1,-1]$ is the metric used within the real-time formalism. The indices are raised and lowered with the metric $\eta^{\mu\nu}$. Here, we assume the velocity in the $xy$ plane to be 1, and we assume the velocity in the $z$ direction to be different, namely, $v_3$. The energy of the fermions is $E_\pm(\boldsymbol{k}) = \pm E(\boldsymbol{k}) = \pm\sqrt{k_x^2 + k_y^2 + v_3^2 k_z^2}$. We should comment that, in this article, we interchangeably use $\mu = (0,1,2,3)$ or $\mu = (t,x,y,z)$ to indicate the time and space directions. The former is algebraically convenient, while the latter is more descriptive and intuitive.

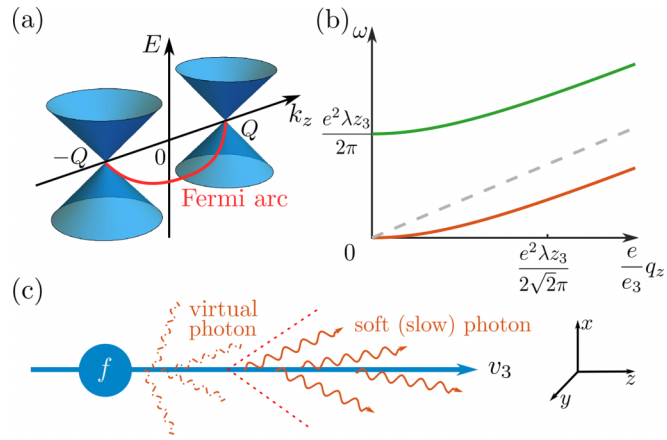


FIG. 1. Low-energy dispersions for (a) free WSM. (b) Photons in the modified electrodynamics with $q_x = q_y = 0$. (a) Around two Weyl nodes, fermions have linear dispersion. The two Weyl nodes are separated in momentum space by $2Q = \lambda z_3$ in the $z$ direction. On the sample boundary, there is a Fermi arc connecting two Weyl nodes, an indication of the anomalous Hall effect. (b) There are two photon modes. The gapped mode (green) has a gap given by $\frac{e^2\lambda z_3}{2\pi}$. The other mode is soft (red), with a quadratic dispersion, Eq. (5). The gray dashed line corresponds to $\omega = \frac{e}{e_3}q_z$, namely, the photon dispersion when $\lambda = 0$. (c) Cartoon of fermions moving in a soft electromagentic environment. Fast-moving fermions constantly interact with virtual photons (red dashed-dotted lines) and spontaneously emit soft photons (red solid lines). The emitted soft photons are roughly confined around the $z$ axis indicated by the red dashed lines.

One should notice that the simplicity in Eq. (2) is deceptive. Indeed, when a lattice model of WSM is considered, the two Weyl components of a Dirac fermion are separated in the Brillouin zone [7], as shown in Fig 1(a). As a result, there will be chiral edge states for a finite-size system. The intersection of the chiral edge state and the Fermi level is the Fermi arc, which is a hallmark of WSMs [8,9]. In terms of transport, the features just mentioned imply that WSMs show an anomalous Hall conductivity [7,10,11,35]. The anomaly argument requires the value of the Hall conductivity to be given by $2\boldsymbol{Q}$, even though high-energy fermions may be strongly interacting with no well-defined quasiparticles [18,26].

Due to the Hall effect, the Lagrangian for the emergent $U(1)$ gauge field has a Chern-Simons (CS)-like term, in addition to the Maxwell term [20]:

$$\mathcal{L}_{\rm M} = -\frac{1}{4e^2}f_{ij}f^{ij} - \frac{1}{2e_3^2}f_{iz}f^{iz}, \tag{3a}$$

$$\mathcal{L}_{\text{CS-like}} = \frac{\lambda z_3}{4\pi}\epsilon^{3ijk}a_i\partial_j a_k, \tag{3b}$$

where $\epsilon^{3ijk}$ is the total antisymmetric tensor in $(3+1)$ dimensions with one index fixed and $i,j,k = 0,1,2$ labels time as well as the $x$ ($y$) direction. $a_\mu$ is the dynamical gauge field potential and $f_{\mu\nu} = \partial_\mu a_\nu - \partial_\nu a_\mu$ is the corresponding field strength tensor. Here, two coupling constants, $e$ and $e_3$, are introduced. As a result, the Maxwell term, Eq. (3a), is anisotropic. The Chern-Simons term, Eq. (3b), introduces more anisotropy, as discussed below.

The second line, Eq. (3b), is the CS-like term and is responsible for the Hall effect. In this work, $z_3$ is essentially the reciprocal lattice constant along the $z$ direction. As shown in Fig. 1(a), $2Q = \lambda z_3$ measures the separation between Weyl points in momentum space. We should mention that to emphasize the anomaly aspect, the CS-like term is sometimes compactly written as $\mathcal{L}_{\text{CS-like}} \sim z \wedge a \wedge da$ in terms of differential forms and the translation gauge field $z_\mu = (0, 0, 0, z_3)$ [26,27]. Indeed, the CS-like term dictates the mixed unquantized anomaly of translation and $U(1)$ gauge symmetry. The mixed anomaly is a manifestation of the chiral anomaly. As we point out, the dynamical effect is also important. Namely, the CS-like term significantly alters the photon dispersion, which in turn influences the properties of the fermions as well as the infrared description of an emergent WSM.

The photon dispersions can be straightforwardly found based on the Euler-Lagrange equation for the $U(1)$ gauge field Lagrangian, Eq. (3). There are two propagating photon modes with the following dispersion relation [20]:

$$\omega_\pm^2 = q_x^2 + q_y^2 + \frac{e^2}{e_3^2} q_z^2 + e^4 \frac{\lambda^2 z_3^2}{8\pi^2} \pm e^4 \frac{\lambda^2 z_3^2}{8\pi^2} \sqrt{1 + 2 \frac{8\pi^2}{e^4 \lambda^2 z_3^2} \frac{e^2}{e_3^2} q_z^2}. \tag{4}$$

When the CS-like term vanishes, $\lambda = 0$, the photons retain a linear dispersion as usual, with an anisotropy in the speed of light: the speed of light in the $xy$ plane is unity, while in the $z$ direction $c_z = \frac{e}{e_3}$.

The presence of the CS-like term, $\lambda \neq 0$, significantly alters the photon dispersion. As plotted in Fig. 1(b), there are two photon modes: a gapped mode as well as a gapless soft mode. The gapped photon mode has the gap $e^2 \frac{\lambda z_3}{2\pi}$. Notice that the gap only depends on the coupling $e^2$, not $e_3^2$. This mode mimics the gapped mode of Maxwell-Chern-Simons theory in $(2+1)$ dimensions [34].

The other photon mode is gapless and quite soft. At low energy, the soft photon takes the following dispersion:

$$\omega_-^2 \approx q_x^2 + q_y^2 + \frac{4\pi^2}{e_3^4 \lambda^2 z_3^2} q_z^4. \tag{5}$$

Namely, the soft photon dispersion is extremely anisotropic due to the CS-like term, Eq. (3b). When moving along the $z$ direction, the photon has a quadratic dispersion with an effective inertia mass $m_s \sim e_3^2 \lambda z_3$. Notice that only $e_3^2$ (not $e^2$) enters the low-energy dispersion at leading order. Such a soft nature will play a central role in our subsequent analysis.

Finally we consider the fermions and the photons to be minimally coupled:

$$\mathcal{L}_c = \bar{\psi}\, \mathcal{V}^\mu a_\mu \psi. \tag{6}$$

Equations (2), (3), and (6) form our full Lagrangian. Such a Lagrangian captures all the essential infrared (IR) features of an emergent WSM, while containing only a limited number of parameters.

The coupling between the fermions and the photons puts some dynamical constraint on the kinematics. In the absence of the CS-like term, Eq. (3b), the fermion velocity and the speed of light renormalizes to be identical in all directions [36]. The same holds true for the velocities in the $xy$ plane when the CS-like term is present. The renormalization effect is more relevant when the gauge field is emergent, in which case the typical velocities of photons and fermions are actually comparable [34]. Based on the considerations just mentioned, we have assumed the velocities of both fermions and photons in the $xy$ plane to be unity. A more drastic effect occurs for the motion in the $z$ direction.

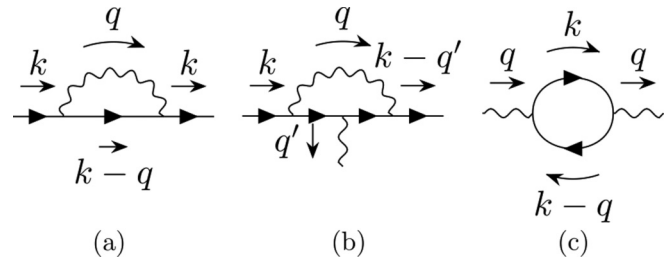


FIG. 2. One-loop diagrams: (a) fermion self-energy, (b) interaction vertex correction, and (c) polarization operator.

A cartoon of fermions moving in the $z$ direction is depicted in Fig. 1(c). In an emergent WSM, the linearly dispersive fermions and the soft photon coexist and are coupled. In the $z$ direction, the fermions move much faster than the photons at low energy. There are two major effects following from this observation.

One effect is related to the photon dressing of the fermion dispersion. Namely, fermions constantly emit and absorb virtual photons [Fig. 1(c)]. Pictorially, the fermions constantly "hit," in particular, the soft photons. Because of the slow velocity, the soft photons serve as an impedance of the fermion motion in the $z$ direction. Therefore, one would expect that the fermion would be dressed by the soft photons and the velocity in the $z$ direction would be reduced.

Another effect is that fermions can radiate photons spontaneously. As schematically shown in Fig. 1(c), the radiated photons are all soft, with the momentum roughly confined in a cone structure around the $z$ axis. This is exactly the picture of Cherenkov radiation in classical electrodynamics [37,38]. Thus, the fermions will acquire a finite lifetime. As we show later, the inverse of the fermion lifetime is proportional to its energy and the fine-structure constant.

In conclusion, we expect that the soft photon renormalizes the fermion velocity in the $z$ direction and gives the fermion a finite lifetime. Such an expectation is supported by the quantum mechanical one-loop calculations as detailed in Sec. III. In the end, the emergent WSM represents an unconventional quantum liquid, whose infrared properties differ significantly from the noninteracting WSM or the standard QED. The unconventional features are the result of the CS-like term, namely, the mixed unquantized anomaly of the WSM.

## III. IMPLICATIONS FROM 1-LOOP DIAGRAMS

In this section, we show that the qualitative picture developed in Sec. II is supported by quantum mechanical calculation. In particular, we study the one-loop diagrams in Fig. 2 as in the standard QED [1,2]. More technical details can be found in the Supplemental Material [32].

We first investigate the full set of the one-loop diagrams (Fig. 2). We show that both the fermion velocity, $v_3$, and the Maxwell speed of light, $c_z = e/e_3$, in the $z$ direction renormalize to zero. At the same time, the electromagnetic coupling constants renormalize to zero. Namely, in the IR limit, the photon dressed fermions are noninteracting and show an asymptotic two-dimensional (2D) dispersion.

Then, we study the imaginary part of the fermion self-energy [Fig. 2(a)]. We show that the inverse of the fermion lifetime (and equivalently the one-photon emission rate) is proportional to the fermion energy. At weak (and even moderate) coupling, the proportionality vanishes logarithmically in the IR limit due to the RG effect. The associated photon radiation process is the quantum version of Cherenkov radiation for the modified electrodynamics of Eq. (3) [38]. Besides, we should mention that the fermion lifetime is also sensitive to the direction of the fermion momentum. Therefore, the emergent WSM represents an unconventional quantum liquid. Over a wide energy range, it behaves like a marginal Fermi liquid, yet with a well-controlled IR behavior.

Before proceeding, it is worthwhile to discuss the typical energy scales. There are three typical energy scales in the current setup. One is $\Lambda_\mathrm{f} \sim v_3\lambda z_3$. Below $\Lambda_\mathrm{f}$, the linear approximation of fermion dispersion, Eq. (2), applies. Second is the photon gap, $m_\mathrm{p} \sim e^2\lambda z_3$, below which the gapped photon mode decouples from the rest of the fields. The last one is slightly subtler: at low enough energy, the photon mode $a_{x,y}$, with quadratic dispersion in $\hat{z}$, $\omega_\mathrm{ph} \sim q_z^2/2m_s$, with inertia mass $m_\mathrm{s} \sim e_3^2\lambda z_3$, and the fermions, with linear dispersion $\omega_f \sim v_3 k_3$, will not be able to couple efficiently due to a large energy mismatch when $q_3$ is comparable to $k_3$. This kinematic constraint leads to the dynamical decoupling of the quadratic-dispersing photon mode with other fields in the theory, which happens when the energy scale is below $m_s v_3^3 \sim v_3^2 e_3^2 \lambda z_3$. Below we work with the energy scale $\Lambda \ll \mathrm{Min}\{\Lambda_\mathrm{f}, m_\mathrm{p}, m_\mathrm{s} v_3^2\}$.

With such a small energy scale (and the corresponding long wavelength), the photon propagator is primarily given by

$$G^\mathrm{a}_{\mu\nu}(q) = e_3^2 \frac{1}{q_0^2 - q_1^2 - q_2^2} \frac{z_\mu z_\nu}{z_3^2}, \tag{7}$$

where $z_\mu = (0, 0, 0, z_3)$. The corrections are on the order of $O(q/m_\mathrm{p,s}) \ll 1$. There is also dependence on the gauge fixing parameter, which may not be small in magnitude. One useful gauge fixing term is given by $\mathcal{L}_\mathrm{gf} = \frac{1}{2}\xi(\partial_i a^i + \frac{e^2}{e_3^2}\partial_z a^z)^2$, with $\xi$ being the gauge fixing parameter [32]. Nevertheless, the gauge fixing parameter does not enter any physical properties, as generally expected from the gauge invariance principle.

One last ingredient is the fermion propagator:

$$G_\mathrm{f}(k) = \frac{\mathcal{V}^\mu k_\mu}{k_0^2 - k_1^2 - k_2^2 - v_3^2 k_3^2}. \tag{8}$$

Notice that both the gauge field and the fermion propagator show some anisotropy. The anisotropy in the gauge field propagator is more important. Indeed, at low energy, only one pole is present in Eq. (7). This pole exactly corresponds to the soft photon at low energy and long wavelength. (Notice that $q_z$ dependence of the soft photon dispersion in Eq. (5) is now subleading and neglected.) Therefore, the unconventional behaviors of the emergent WSM reported in this section are indeed due to the soft photon.

### A. Fermion velocity renormalization and the RG equations

For weak interaction, the fermionic excitations are presumably underdamped. Then, we can ask the question of how fermion band structure renormalizes. Along the $z$ direction, the fast-moving fermions are dressed by the slow-moving photons due to the interaction. Therefore, a reduction in the fermion velocity $v_3$ is expected from the RG analysis.

To be more specific, we aim at the renormalization of the dispersion of fermions and photons as well as the coupling strength between them. Namely, we would like to obtain the RG flow of $v_3$, $e$, and $e_3$. To achieve this goal, the following bare scaling dimension is considered:

$$[k_\mu] = [q_\mu] = 1,\ [\bar{\psi}] = [\psi] = \tfrac{3}{2},\ [a_\mu] = 1. \tag{9}$$

Under this bare scaling, the CS-like term, Eq. (3b), is relevant. Meanwhile, all the other terms in the Lagrangian, Eqs. (2), (3a), and (6), are marginal. The relevance of the CS-like term implies that all the three typical scales, $\Lambda_\mathrm{f}$, $m_\mathrm{p}$, and $m_\mathrm{s} v_3^2$, renormalize to infinity. This is indeed the case when we consider the full RG equation below. The relevance of the three typical energy scales is also reflected in the gauge field propagator. As shown in Eq. (7), at low energy, only one pole at $q_0^2 = q_1^2 + q_2^2$ is present in the leading-order term of the gauge field propagator.

The fermion velocity renormalization can be obtained from either the fermion self-energy, $\Sigma(k)$ in Fig. 2(a), or the vertex correction, $\Gamma^\mu(k, q')$ in Fig. 2(b). The two diagrams are related by the Ward identity. In particular, we focus on the following quantity [1,2]:

$$\Gamma^\mu_{\text{1-loop}}(k, q' = 0)|_{k=0} = -\partial_{k_\mu}\Sigma(k)|_{k=0.} \tag{10}$$

Combined with the bare interaction vertex, Eq. (6), the full interaction vertex is given by

$$\Gamma^\mu_\mathrm{full}(k, q' = 0)|_{k=0} = Z_\mathrm{f}^{-1}[\gamma^0, \gamma^1, \gamma^2, \tilde{v}_3\gamma^3], \tag{11}$$

where all the gauge fixing parameters enter the fermion field renormalization factor $Z_\mathrm{f}$. As a result, the effective velocity $\tilde{v}_3$ is independent of the gauge fixing parameter:

$$\tilde{v}_3 = v_3 - \frac{e_3^2}{6\pi^2}\frac{v_3^3}{|v_3|}\ln\frac{\Lambda}{\mu_\mathrm{IR}}, \tag{12}$$

where $\Lambda$ and $\mu_\mathrm{IR}$ are the UV and IR cutoff in the loop momentum integral. This result suggests that the fermion velocity $v_3$ is reduced by the photon dressing.

The renormalization of the coupling constants $e$ and $e_3$ can be obtained from the vacuum polarization $\Pi^{\mu\nu}(q)$ as in Fig. 2(c). Technically, the vacuum polarization is evaluated with the dimensional regularization scheme, in order to maintain gauge invariance [1,2]. Assuming the space-time dimension as $d = 4 - \epsilon$, Fig. 2(c) contains a factor of $\Pi^{\mu\nu}(q) \propto \Lambda^\epsilon[\frac{2}{\epsilon} - \ln\Delta^2(q)] \sim \ln\frac{\Lambda^2}{\Delta^2(q)}$, which is reduced to a logarithmically divergent factor by minimal subtraction [32]. Here, $\Delta^2(q) = q_0^2 - q_1^2 - q_2^2 - v_3^2 q_3^2$.

Physically, the vacuum polarization operator [Fig. 2(c)] gives a correction to the bare Maxwell term, Eq. (3a). The

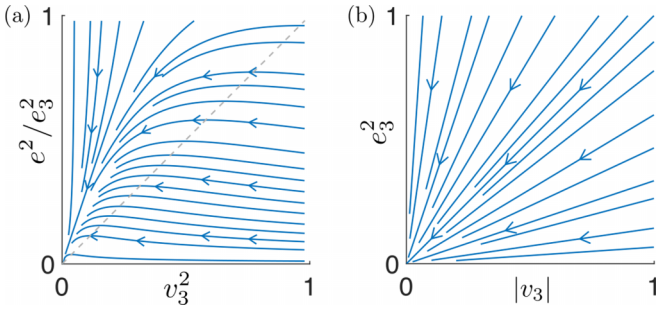


FIG. 3. Renormalization group flow with $N_f = 1$ pair of Weyl fermions.

resultant Lagrangian is of the same form as Eq. (3a), with the effective coupling constants [39]:

$$\frac{1}{\tilde{e}^2} = \frac{1}{e^2} + \frac{N_f}{12\pi^2}\frac{1}{|v_3|}\ln\frac{\Lambda^2}{\Delta^2(q)},$$
$$\frac{1}{\tilde{e}_3^2} = \frac{1}{e_3^2} + \frac{N_f}{12\pi^2}|v_3|\ln\frac{\Lambda^2}{\Delta^2(q)}, \tag{13}$$

where $N_f$ is the number of pairs of the Weyl points. Notice that the CS-like term is unaffected by the vacuum polarization operator. This is because the CS-like term comes from integrating out the high-energy fermionic states away from the Weyl points [18,26], while the polarization operator computed here only involves the low-energy fermions around the Weyl points.

Based on the bare scaling dimension, Eq. (9), and the results of Eqs. (12) and (13), we obtain the main results, namely, the RG equations:

$$\frac{dz_3}{dl} = z_3, \tag{14a}$$
$$\frac{dv_3}{dl} = -\frac{e_3^2}{6\pi^2}\frac{v_3^3}{|v_3|}, \tag{14b}$$
$$\frac{de^2}{dl} = -N_f\frac{e^4}{6\pi^2}\frac{1}{|v_3|}, \quad \frac{de_3^2}{dl} = -N_f\frac{e_3^4}{6\pi^2}|v_3|, \tag{14c}$$

where the RG process is defined through the change in the UV scale as $\Lambda \to \Lambda\exp[-dl]$ with $dl > 0$. The RG equation for the reciprocal lattice constant $z_3$, Eq. (14a), follows from the bare scaling equation (9).

Figure 3 plots the RG flow of a few typical parameters. Figure 3(a) shows the RG flow of the fermion velocity $v_3$ and the speed of light (as defined solely from the Maxwell term) $c_z = e/e_3$. While the fermion velocity always flows to a smaller value, there is a slow increase in $c_z$ when the fermion velocity is large $v_3 > c_z$. Nevertheless, both velocities flow to zero eventually. Figure 3(b) shows that in addition to the reduction of the velocities in the $z$ direction, the coupling constant $e_3$ also flows to zero. From the RG flow, we conclude that, in the deep IR limit, the emergent WSM coupled with the dynamical $U(1)$ gauge field shows asymptotic two-dimensional dispersion and is free of interaction. The weakly coupled IR limit also justifies our perturbative loop expansion.

We should comment on the flow of the three typical energy scales, $\Lambda_f$, $m_p$, and $v_3^2 m_s$. Notice that those scales are of the form $\{v_3, e^2, v_3^2 e_3^2\} \times z_3$. From the RG equation, the fermion velocity and the coupling constants renormalize to zero as $1/\mathrm{PolyLog}(\Lambda)$, as suggested by Eqs. (12) and (13). Meanwhile, the reciprocal lattice constant $z_3$ renormalizes to infinity in a way faster than logarithmic growth, $z_3 \to z_3\exp[l]$. As a result, the three energy scales should renormalize to infinity, as mentioned at the beginning of this subsection. This justifies our assumption that the probing energy scale is always much smaller than $\Lambda_f$, $m_p$, and $v_3^2 m_s$.

The most interesting feature of our result is that the fermion band structure is strongly dressed by the soft photons. In particular, the velocity in the $z$ direction, $v_3$, renormalizes to zero. Such a result matches the qualitative expectation that the soft photons are essentially an impedance of the fermion motion in the $z$ direction. One may wonder about the nonanalyticity of the RG flow equations, Eqs. (12) and (13), at $v_3 = 0$. This is because the momentum shell at the cutoff $\Lambda^2 = q_0^2 + q_1^2 + q_2^2 + v_3^2 q_3^2$, as a surface in momentum space, has different topology for $v_3 \neq 0$ (ellipse) and $v_3 = 0$ (infinite cylinder). The nonanalyticity in $v_3$ also makes the velocity term *dangerously irrelevant* [40], and the limit $v_3 \to 0$ should always be taken with caution, even if one is primarily interested in the fixed point properties.

### B. Photon emission rate and fermion lifetime

The second effect is related to the spontaneous emission of photons and correspondingly the fermion lifetime. As schematically illustrated in Fig. 1(c), when moving in the $z$ direction, fermions can spontaneously emit the soft photons. A comment on the definition of the soft (slow) and fast photon is due. Qualitatively, the criteria amounts to the comparison between the photon's phase velocity $c_{\mathrm{phase}}$ and the fermion's group velocity $v_{\mathrm{group}}$ [37]. When the photon's phase velocity is small $c_{\mathrm{phase}} < v_{\mathrm{group}}$, the photons are soft and slow and can be emitted spontaneously. In the opposite limit, the photons are fast and cannot be emitted. A careful analysis of energy-momentum conservation generally gives a stricter kinematic constraint on the emitted photons.

The one-photon emission rate can be calculated from the imaginary part of the fermion self-energy [Fig. 2(a)] by the optical theorem [1,2,41]. When the external fermions are put on mass-shell, the result of the calculation is fully independent of gauge choice, according to the Ward identity [1,2]. Thus, the imaginary part of the on-mass-shell fermion self-energy is considered in this subsection, $\tau^{-1} = 2\mathrm{Im}\,\mathrm{tr}\Sigma(k)\hat{P}_{\pm}(k)|_{k_0=\pm E(\boldsymbol{k})}$ [32], where $\hat{P}_{\pm}(k)$ is the projection operator onto the positive (negative)-energy fermion bands.

Given the rotation symmetry in the $xy$ plane, we can assume the external fermion has a momentum in the $xz$ plane without loss of generality. Namely, the momentum of the external fermion is $\boldsymbol{k} = |\boldsymbol{k}|(\sin\theta, 0, \cos\theta)$. To leading order in the coupling constant $e_3^2$, we found that the one-photon emission rate or equivalently the inverse fermion lifetime is given by

$$\tau^{-1} = \frac{e_3^2}{3\pi}E(\boldsymbol{k})\frac{|v_3|^3\cos^2\theta}{\sin^2\theta + v_3^2\cos^2\theta}. \tag{15}$$

It is proportional to the fine-structure constant $\frac{e_3^2}{4\pi}$ and the fermion energy $E(\boldsymbol{k}) = |\boldsymbol{k}|\sqrt{\sin^2\theta + v_3^2\cos^2\theta}$. In addition,

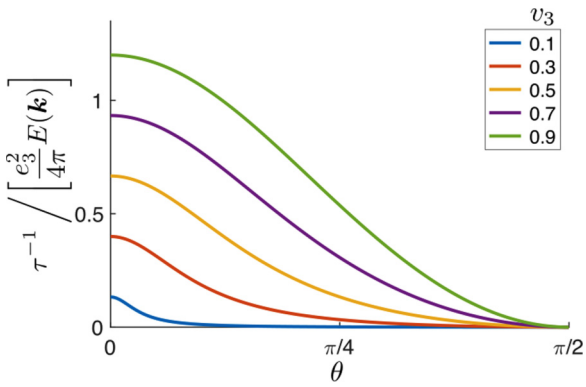


FIG. 4. Inverse fermion lifetime versus the direction of fermion momentum at various values of velocity $v_3$. The fermion has a momentum in the $xz$ plane of $\boldsymbol{k} = |\boldsymbol{k}|(\sin\theta, 0, \cos\theta)$ and energy $E(\boldsymbol{k}) = |\boldsymbol{k}|\sqrt{\sin^2\theta + v_3^2\cos^2\theta}$. Here, the fermion energy is small compared to the typical energy scales in the system.

the fermion lifetime also depends on the fermion velocity and the direction of momentum.

As plotted in Fig. 4, the inverse of the fermion lifetime increases with increasing velocity $v_3$. This matches the expectation of Cherenkov radiation [37]. The inverse lifetime also depends on the direction of the fermion momentum. Indeed, the inverse lifetime is maximum when the fermion moves in the $z$ direction ($\theta = 0$). Meanwhile, the fermions do not emit photons when moving in the $xy$ plane ($\theta = \pi/2$).

At weak coupling, $e_3^2/4\pi \ll 1$, the fermions are indeed underdamped. The presumption of weak damping in the RG analysis is justified. The parameters in Eq. (15) can be thought of as the renormalized ones. The inverse of the fermion lifetime is proportional to its energy, $\tau^{-1} \propto E(\boldsymbol{k})$. Meanwhile, the coefficient of proportionality approaches zero logarithmically upon approaching the IR limit.

In addition, when the coupling strength is moderate, $e_3^2/4\pi \lesssim 1$, the inverse fermion lifetime is still proportional to the energy. The ratio between the two quantities may not be small, $[\tau E(\boldsymbol{k})]^{-1} \lesssim O(1)$. This suggests that the fermions are significantly damped at the moderate electromagnetic coupling. Accordingly, the fermionic quasiparticles are not sharply defined.

We expect the RG still plays some role in the moderate-coupling regime. Then the coupling constants flow to a smaller value. The assumed relevance of the RG implies the emergence of a new energy scale $\Lambda_1$. Above $\Lambda_1$, the fermionic excitations are overdamped as discussed in the previous paragraph. Below $\Lambda_1$, the coupling strength becomes small. The fermionic excitations eventually become weakly interacting or even noninteracting and underdamped. We should mention that the determination of the energy scale $\Lambda_1$ is beyond the scope of the perturbative analysis presented in this article.

Therefore, we conclude that the emergent WSM represents an unconventional quantum liquid. Over a wide energy window above $\Lambda_1$, it behaves like a marginal Fermi liquid and lacks sharply defined quasiparticles [29]. Meanwhile, in the IR limit below $\Lambda_1$, even though the fermionic quasiparticles are well-defined, the dispersion shows an asymptotic two-dimensional feature. This conclusion means that the properties of an emergent Weyl semimetal are significantly different from its mean field description as in Sec. II at both IR and intermediate energy scales.

At strong coupling, the fermionic quasiparticles are overdamped. Then, perhaps a hydrodynamic description for such chiral plasma is in order, which we do not pursue in great detail here.

## IV. CONCLUSION AND DISCUSSIONS

To conclude, we investigate the dynamical effect of the chiral anomaly, through the question of what is the infrared description of an emergent Weyl semimetal. We found that the emergent WSM represents an unconventional quantum liquid. The anomaly term guarantees the softness of the emergent photons. Due to the soft nature of the emergent *U(1)* gauge field, the IR behavior of the emergent WSM is quite distinct from that of the noninteracting WSM in two aspects.

First, the fermions get dressed by the soft photons significantly. The fermion velocity in the $z$ direction renormalizes to zero. In the IR limit, both fermions and gauge fields show an asymptotic 2D dispersion. Meanwhile, the emergent fine-structure constant renormalizes to zero as well, leading to a decoupled IR limit.

Second, the fermions acquire a finite lifetime through spontaneous emission of soft photons. The inverse of the fermion lifetime is found to be proportional to the fine-structure constant and, more interestingly, the fermion energy. This suggests that the emergent WSM behaves like a marginal Fermi liquid at finite energy. However, due to the RG effect, the emergent WSM has a well-controlled (noninteracting) IR limit.

The reported features of an emergent WSM is potentially detectable through specific heat measurement [30,31]. The specific heat of fermions scales with temperature $T$ as $C_\mathrm{f} \sim T^3/|v_3|$. At low-temperature $T \ll m_\mathrm{s}$, the contribution from the soft photons has a different power, $C_\mathrm{sp} \sim m_\mathrm{s}^{1/2} T^{5/2}$. Therefore, it is possible to single out the fermionic contribution to the specific heat [42]. The measurement of fermionic specific heat reveals the velocity renormalization effect. In particular, $C_\mathrm{f}/T^3 \sim 1/|v_3|$ should show a logarithmic increase upon lowering the temperature. Notice that the acoustic phonon in 3D also has a specific heat of cubic temperature dependence, $C_\mathrm{ap} \sim T^3$. We expect the renormalization effect on phonon dispersion is limited. Hence, $C_\mathrm{ap}/T^3$ is basically temperature independent. Therefore, after singling out the emergent photons, an increase in $(C_\mathrm{f} + C_\mathrm{ap})/T^3$ with lowering the temperature should reflect the renormalization effect of reducing the fermion velocity $v_3$ in the IR limit.

## ACKNOWLEDGMENTS

We are grateful to Sung-Sik Lee, Ruochen Ma, Alex Kamenev, Adam Nahum, and Jinmin Yi for the valuable discussions. We acknowledge support from the Natural Sciences and Engineering Research Council (NSERC) of Canada. A.A.B. was also supported by the Center for Advancement of Topological Semimetals, an Energy Frontier Research Center funded by the U.S. Department of Energy, Office of Science, Office of Basic Energy Sciences, through the

Ames Laboratory under Contract No. DE-AC02-07CH11358. Research at the Perimeter Institute is supported in part by the Government of Canada through the Department of Innovation, Science and Economic Development, and by the Province of Ontario through the Ministry of Economic Development, Job Creation and Trade.

[1] S. Weinberg, *The Quantum Theory of Fields* (Cambridge University, Cambridge, England, 1995), Vol. 1.
[2] M. E. Peskin and D. V. Schroeder, *An Introduction to Quantum Field Theory* (Addison-Wesley, Reading, MA, 1995).
[3] G. E. Volovik, *The Universe in a Helium Droplet* (Clarendon, Oxford, 2003).
[4] H. B. Nielsen and M. Ninomiya, Phys. Lett. B **130**, 389 (1983).
[5] H. B. Nielsen and M. Ninomiya, Nucl. Phys. B **185**, 20 (1981).
[6] H. B. Nielsen and M. Ninomiya, Nucl. Phys. B **193**, 173 (1981).
[7] A. A. Burkov and L. Balents, Phys. Rev. Lett. **107**, 127205 (2011).
[8] B. Q. Lv, H. M. Weng, B. B. Fu, X. P. Wang, H. Miao, J. Ma, P. Richard, X. C. Huang, L. X. Zhao, G. F. Chen, Z. Fang, X. Dai, T. Qian, and H. Ding, Phys. Rev. X **5**, 031013 (2015).
[9] S.-Y. Xu, I. Belopolski, N. Alidoust, M. Neupane, G. Bian, C. Zhang, R. Sankar, G. Chang, Z. Yuan, C.-C. Lee, S.-M. Huang, H. Zheng, J. Ma, D. S. Sanchez, B. Wang, A. Bansil, F. Chou, P. P. Shibayev, H. Lin, S. Jia, and M. Z. Hasan, Science **349**, 613 (2015).
[10] N. P. Armitage, E. J. Mele, and A. Vishwanath, Rev. Mod. Phys. **90**, 015001 (2018).
[11] A. A. Zyuzin and A. A. Burkov, Phys. Rev. B **86**, 115133 (2012).
[12] F. de Juan, A. G. Grushin, T. Morimoto, and J. E. Moore, Nat. Commun. **8**, 15995 (2017).
[13] H. Isobe and N. Nagaosa, Phys. Rev. Lett. **116**, 116803 (2016).
[14] C. Rylands, A. Parhizkar, A. A. Burkov, and V. Galitski, Phys. Rev. Lett. **126**, 185303 (2021).
[15] Z. Wang and S.-C. Zhang, Phys. Rev. B **87**, 161107(R) (2013).
[16] J. Maciejko and R. Nandkishore, Phys. Rev. B **90**, 035126 (2014).
[17] E. Sagi, A. Stern, and D. F. Mross, Phys. Rev. B **98**, 201111(R) (2018).
[18] C. Wang, L. Gioia, and A. A. Burkov, Phys. Rev. Lett. **124**, 096603 (2020).
[19] M. Thakurathi and A. A. Burkov, Phys. Rev. B **101**, 235168 (2020).
[20] S. M. Carroll, G. B. Field, and R. Jackiw, Phys. Rev. D **41**, 1231 (1990).
[21] F. Hotz, A. Tiwari, O. Turker, T. Meng, A. Stern, M. Koch-Janusz, and T. Neupert, Phys. Rev. Res. **1**, 033029 (2019).
[22] T. Meng, A. G. Grushin, K. Shtengel, and J. H. Bardarson, Phys. Rev. B **94**, 155136 (2016).
[23] W. Witczak-Krempa, M. Knap, and D. Abanin, Phys. Rev. Lett. **113**, 136402 (2014).
[24] O. Türker and T. Meng, SciPost Phys. **8**, 031 (2020).
[25] A. G. Grushin, Phys. Rev. D **86**, 045001 (2012).
[26] L. Gioia, C. Wang, and A. A. Burkov, Phys. Rev. Res. **3**, 043067 (2021).
[27] C. Wang, A. Hickey, X. Ying, and A. A. Burkov, Phys. Rev. B **104**, 235113 (2021).
[28] M. Levin and M. P. A. Fisher, Phys. Rev. B **79**, 235315 (2009).
[29] C. M. Varma, P. B. Littlewood, S. Schmitt-Rink, E. Abrahams, and A. E. Ruckenstein, Phys. Rev. Lett. **63**, 1996 (1989).
[30] M. Sitte, A. Rosch, J. S. Meyer, K. A. Matveev, and M. Garst, Phys. Rev. Lett. **102**, 176404 (2009).
[31] S. Dzsaber, L. Prochaska, A. Sidorenko, G. Eguchi, R. Svagera, M. Waas, A. Prokofiev, Q. Si, and S. Paschen, Phys. Rev. Lett. **118**, 246601 (2017).
[32] See Supplemental Material at http://link.aps.org/supplemental/10.1103/PhysRevB.107.035131 for detailed discussion of (i) the gauge fixing term, (ii) the gauge field propagator, (iii) the one-loop vertex correction, (iv) the vacuum polarization operator, and (v) the fermion self-energy and lifetime.
[33] P. A. Lee, N. Nagaosa, and X.-G. Wen, Rev. Mod. Phys. **78**, 17 (2006).
[34] X.-G. Wen, *Quantum Field Theory of Many-Body Systems: From the Origin of Sound to an Origin of Light and Electrons* (Oxford University, Oxford, 2004).
[35] A. A. Burkov, Phys. Rev. Lett. **113**, 187202 (2014).
[36] M. M. Anber and J. F. Donoghue, Phys. Rev. D **83**, 105027 (2011).
[37] J. Schwinger, L. L. DeRaad, Jr., K. A. Milton, and W.-Y. Tsai, *Classical Electrodynamics* (Westview, Boulder, CO, 1998).
[38] K. Tuchin, Phys. Rev. D **98**, 114026 (2018).
[39] A. Zee, *Quantum Field Theory in a Nutshell*, Nuclear Physics in a Nutshell (Princeton University, Princeton, NJ, 2010), Vol. 7.
[40] J. Cardy, *Scaling and Renormalization in Statistical Physics*, Cambridge Lecture Notes in Physics (Cambridge University, Cambridge, England, 1996), Vol. 5.
[41] A. Kamenev, *Field Theory of Non-equilibrium Systems* (Cambridge University, Cambridge, England, 2011).
[42] C. Kittel, *Introduction to Solid State Physics*, 8th ed. (Wiley, New York, 2005).